

## Defect-enhanced anomaly in frequency synchronization of asymmetrically coupled spatially extended systems

J. Bragard,<sup>1,\*</sup> E. Montbrió,<sup>2</sup> C. Mendoza,<sup>1,3</sup> S. Boccaletti,<sup>3</sup> and B. Blasius<sup>2</sup>

<sup>1</sup>*Department of Physics and Applied Mathematics, Universidad de Navarra, E31080 Pamplona, Spain*

<sup>2</sup>*Institut für Physik, Universität Potsdam, D-14469 Potsdam, Germany*

<sup>3</sup>*Istituto Nazionale di Ottica Applicata, Largo E. Fermi, 6 I50125 Florence, Italy*

(Received 25 June 2004; published 9 February 2005)

We analytically establish and numerically show that anomalous frequency synchronization occurs in a pair of asymmetrically coupled chaotic space extended oscillators. The transition to anomalous behaviors is crucially dependent on asymmetries in the coupling configuration, while the presence of phase defects has the effect of enhancing the anomaly in frequency synchronization with respect to the case of merely time chaotic oscillators.

DOI: 10.1103/PhysRevE.71.025201

PACS number(s): 05.45.Xt, 05.45.Gg, 05.45.Jn

In recent years, synchronization of complex systems have generated great interest in the scientific community [1], as well as in the literature oriented to lay audiences [2]. A relevant and counterintuitive result is that an increase in coupling strength between two complex systems does not necessarily induce a better degree of synchronization. An example is the anomalous behavior observed in the frequency synchronization between a limit cycle and a time chaotic oscillator [3,4], where increasing the coupling leads initially to an increase of the frequency difference.

In this paper we analytically establish and numerically show that: (i) anomalous frequency synchronization (AFS) is a generic phenomenon occurring also for space extended systems, (ii) the transition to anomalous behaviors is crucially dependent on asymmetries in the coupling configuration, and (iii) the presence of phase defects in spatially extended chaotic oscillators has the role of enhancing the anomaly in frequency synchronization with respect to the case of merely time chaotic oscillators.

Our starting point is a pair of asymmetrically coupled complex Ginzburg-Landau equations (CGLE)

$$\begin{aligned} \dot{A}_{1,2} = & A_{1,2} + (1 + i\alpha)\partial_{xx}A_{1,2} - (1 + i\beta_{1,2})|A_{1,2}|^2A_{1,2} \\ & + \frac{c}{2}(1 \mp \theta)(A_{2,1} - A_{1,2}). \end{aligned} \quad (1)$$

Here  $A_{1,2}(x, t) = \rho_{1,2}(x, t)e^{i\phi_{1,2}(x, t)}$  are two one-dimensional complex fields [of amplitudes  $\rho_{1,2}(x, t)$  and phases  $\phi_{1,2}(x, t)$ ], the dots denote temporal derivatives,  $\partial_{xx}$  stays for the second derivative with respect to the space variable  $0 \leq x \leq L$ ,  $L$  is the system extension,  $\alpha$  and  $\beta_{1,2}$  are suitable real parameters,  $c$  represents the coupling strength, and  $-1 \leq \theta \leq 1$  is a parameter accounting for asymmetries in the coupling. CGLE has been extensively investigated in the context of space-time chaos, since it describes the universal dynamical features of an extended system close to a Hopf bifurcation [5]. A detailed account of CGLE dynamics and synchronization phe-

nomena can be found in Ref. [6]. In particular, Eq. (1) supports two main turbulent regimes, namely phase turbulence (PT) and amplitude turbulence (AT) or defect turbulence [7]. PT is a regime where the chaotic behavior of the field is essentially dominated by the dynamics of  $\phi(x, t)$ , while the amplitude changes smoothly, and it is always bounded away from zero. At variance, in AT the fluctuations of  $\rho(x, t)$  become dominant over the phase dynamics, leading to large amplitude oscillations that can occasionally cause the occurrence of a space-time defect in the point where  $\rho$  is locally vanishing. In Ref. [6] we have numerically shown that when coupling a PT and a AT regime, one can have regular frequency synchronization (FS) or AFS, depending upon the value of the asymmetry parameter. In this paper, we will concentrate on the case in which both CGLE are initially (for  $c=0$ ) set in a regime of phase turbulence (PT), i.e., we fix the parameters in Eq. (1) to be  $\alpha=2$ ,  $\beta_1=-0.75$ , and  $\beta_2=-0.9$ . This will indeed allow us to perform a detailed analytical study of the synchronization process, and to rigorously describe the main dynamical and statistical features characterizing AFS. Here, the condition to be fulfilled for 1:1 frequency synchronization is the vanishing of the mean frequency mismatch  $\Delta\Omega \equiv \Omega_1 - \Omega_2 = 0$ , where the mean frequency of each field is given by  $\Omega_{1,2} = \lim_{t \rightarrow \infty} (\langle \phi_{1,2}(x, t) \rangle_x) / t$  ( $\langle \cdot \rangle_x$  denoting spatial average).

Figure 1 reports  $\Delta\Omega$  in the parameter space  $(c, \theta)$  and indicates that the transition to a frequency locked state ( $\Delta\Omega=0$ ) can occur in a regular ( $\Delta\Omega$  is a monotonically decreasing function of  $c$ ) or in an anomalous way ( $\Delta\Omega$  increases initially with  $c$ ), depending upon the level of asymmetry in the coupling configuration. The arrow in Fig. 1 indicates the critical value  $\theta_{cr} \approx -0.09$  and marks the numerically found transition point between the two frequency synchronization behaviors.

Since both fields are initially set in the PT regime, we can use the tools of asymptotic analysis in order to reduce the description to a pair of coupled Kuramoto-Sivashinsky (KS) equations [8]. The KS model is nothing but an ordinary differential Ginzburg-Landau (GL) model plus spatial terms that are “small” perturbations. In the following we will evaluate such small perturbations and show that their probability distribution function (PDF) is very well approximated

\*Electronic address: [jbragard@fisica.unav.es](mailto:jbragard@fisica.unav.es)

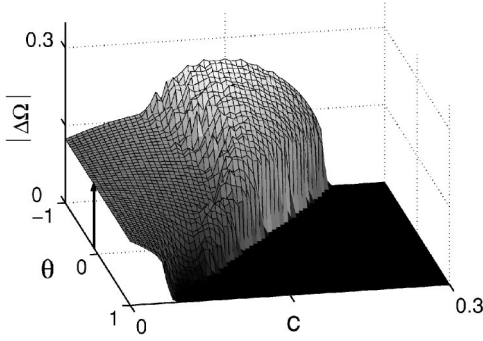


FIG. 1. Frequency mismatch  $|\Delta\Omega|$  vs the parameter space  $(c, \theta)$  for Eq. (1). All parameters are specified in the text. The arrow pointing at  $\theta_{cr} \approx -0.09$  discriminates between regular ( $\theta_{cr} < \theta \leq 1$ ) and anomalous ( $-1 \leq \theta < \theta_{cr}$ ) frequency synchronization.

by a Gaussian distribution, whose mean and standard deviation depend on the parameters  $\alpha$  and  $\beta$ . This allows one to perform a second reduction leading to a pair of ordinary differential GL equations with suitable additive noise terms, and compare the prediction from this latter model with the results of the full CGLE, thus gathering a better understanding of the mechanisms behind AFS in spatially extended systems.

Let us start with a single CGLE equation; the coupling will be added later on. The equation is

$$\dot{A} = A + (1 + i\alpha)\partial_{xx}A - (1 + i\beta)|A|^2A. \quad (2)$$

In the PT regime, the dynamics of the complex field  $A(x, t)$  can be reduced to the dynamics of the real phase field  $\phi(x, t)$ , being the amplitude field  $\rho(x, t)$  slaved to the dynamics of the phase. The family of equations that describe the dynamics of the phase equations are called the Kuramoto-Sivashinsky equations [9]. Such equations have been found to properly describe chemical reactions (e.g., Belousov-Zhabotinsky reaction) as well as flame propagation in the case of mild combustion. The equation for the phase dynamics of the single CGLE has been derived by Sakaguchi [10] and reads as

$$\dot{\phi} = t_1\phi_{xx} + t_2\phi_x^2 + t_3\phi_{xxx} + t_4\phi_x\phi_{xx} + t_5\phi_{xx}^2 + t_6\phi_x^2\phi_{xx}, \quad (3)$$

where  $t_1 = 1 + \alpha\beta$ ,  $t_2 = \beta - \alpha$ ,  $t_3 = -\alpha^2(1 + \beta^2)/2$ ,  $t_4 = -2\alpha(1 + \beta^2)$ ,  $t_5 = -\alpha(1 + \beta^2)$ , and  $t_6 = -2(1 + \beta^2)$ . Equation (3) is obtained by doing an asymptotic expansion of Eq. (2) in powers of  $\partial_x$ , the smallness parameter being the degree of spatial modulation of the phase.

By using the Adams-Bashforth integration scheme, both Eq. (2) and Eq. (3) have been simulated with the same grid spacing  $\delta x = 0.25$ , with time step  $\delta t = 10^{-2}$ , and with periodic boundary conditions. As initial condition for Eq. (3), we selected a Gaussian noise with zero mean and standard deviation  $\sigma = 10^{-4}$ . In Eq. (3), after some transient, the phase  $\phi$  is drifting linearly with time ( $\langle \phi \rangle_x \approx st + b$ , where  $s$  is the slope of the linear drift evaluated by performing a linear fit). The validity of the KS model is then checked by comparing the average frequency obtained from the full CGLE [Eq. (2)]

and the frequency estimate given by the KS model  $\omega = -\beta + s$ . An excellent agreement has been obtained for the frequencies calculated with the two models (KS and full CGLE) in the whole PT regime ( $-0.9 < \beta < -0.7$ ).

In fact, as we are interested in a first-order perturbation theory, we can limit ourselves to the first three terms in the right-hand side of Eq. (3), and still we have verified that the agreement between the average frequencies calculated from the full CGLE and the three-terms KS equation is very good in the whole PT range.

The advantage of the three-terms reduction of Eq. (3) is that it is now straightforward to perform a spatial average of such reduced equation, that leads to

$$\langle \dot{\phi} \rangle_x = t_2 \langle \phi_x^2 \rangle_x. \quad (4)$$

Equation (4) is a very simple relationship for the correction to the frequency (we recall that  $\omega = -\beta + \langle \dot{\phi} \rangle_x$ ). In Fig. 2(a), the time evolution of the term  $\langle \phi_x^2 \rangle_x$  (from now on referred to as T2) is displayed, as it is taken from the simulation of the full CGLE. The time evolution of T2 is clearly chaotic and its probability distribution function (PDF) can be conveniently fitted by a Gaussian [as shown in Fig. 2(b)]. Furthermore, the time correlation function for T2 is reported in Fig. 2(c). There, by assuming an exponential decay, we obtain an estimate for the correlation time of  $\tau = 51.2$ .

Such statistical properties make it possible to further reduce our analysis to a pair of time-dependent coupled oscillators (GL equations) subjected to a colored Gaussian noise with proper mean, fluctuation, and correlation features [for  $\beta_1 = -0.75$  ( $\beta_2 = -0.9$ ) we have that the mean of the PDF is  $\mu_1 = 2.92 \times 10^{-3}$  ( $\mu_2 = 1.14 \times 10^{-2}$ ), the standard deviation is  $\sigma_1 = 5.46 \times 10^{-4}$  ( $\sigma_2 = 1.7 \times 10^{-3}$ ), and the correlation time is  $\tau_1 = 51.2$  ( $\tau_2 = 15.3$ )]. Notice that as  $\beta$  is increased (in absolute value), the system becomes more and more chaotic, thus the correction to the frequency is larger (as indicated by a larger  $\mu$ ), the fluctuations are higher (as indicated by a larger  $\sigma$ ), and the correlation time of the signal decays (as confirmed by a lower value of  $\tau$ ).

Taking back into account the coupling term, using proper noise terms and assuming small parameter mismatches, the reduced GL model [3,11] for the phases  $\phi_1(t)$ ,  $\phi_2(t)$  of the chaotic oscillators becomes

$$\dot{\phi}_1 = -\beta_1 - c_1[\beta_1(\cos \varphi - 1) - \sin \varphi] + \eta_1,$$

$$\dot{\phi}_2 = -\beta_2 - c_2[\beta_2(\cos \varphi - 1) + \sin \varphi] + \eta_2, \quad (5)$$

where  $\varphi = \phi_2 - \phi_1$  represents the phase difference between the two oscillators,  $c_1 = c(1 - \theta)/2$ ,  $c_2 = c(1 + \theta)/2$ , and  $\eta_1, \eta_2$  are the two colored Gaussian noise terms specified above. Equations (5) are a set of stochastic differential equations (SDE), where the noise terms  $\eta_1, \eta_2$  have been surrogated from the full CGLE with the corresponding parameters  $\alpha, \beta$ , and  $c = 0$  (uncoupled). The numerical integration of the set of Eqs. (5) is straightforward [12,13] and allows us to compare the full CGLE to its SDE counterpart.

Before proceeding with numerical integration, some analytical studies of Eqs. (5) can be performed, following what

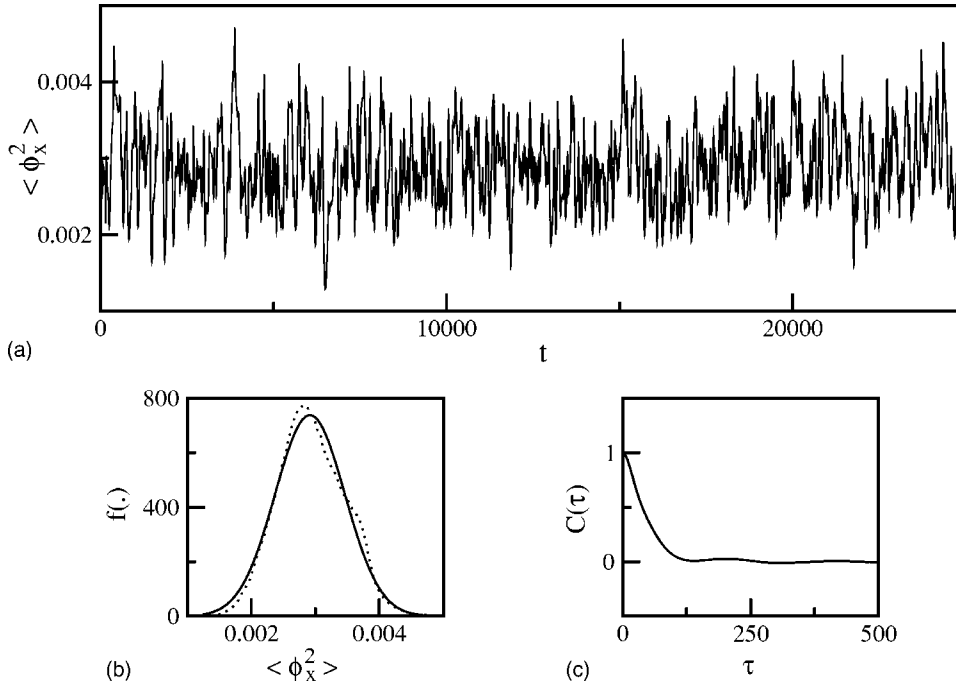


FIG. 2. (a) Time evolution of  $\langle \phi_x(x, t)^2 \rangle_x$  from Eq. (2) with  $\alpha = 2$  and  $\beta = -0.75$ . For a better statistics, nine different random initial conditions have been considered, and the integration lasts until  $t = 10^6$ . (b) The probability distribution function of the data shown in (a) (dotted line) and its fit by a Gaussian PDF (solid line). (c) The time correlation function of the signal shown in (a).

was done in Ref. [4]. Namely, by neglecting the noise terms and subtracting Eqs. (5), one is able to write an equation for  $\dot{\phi}$  in a closed form. Then frequency synchronization is studied by calculating the frequency detuning,  $(\Delta\Omega)^{-1} = 1/2\pi \int_0^{2\pi} d\varphi / \dot{\varphi}$ , yielding

$$|\Delta\Omega| = \sqrt{B_-^2 + cB_-[\theta B_+ - B_-] + c^2}, \quad (6)$$

where  $B_+$  ( $B_-$ ) stays for  $\beta_1 + \beta_2$  ( $\beta_1 - \beta_2$ ). The interest of expression (6) is that one can analytically estimate the transition point between FS and AFS. Indeed, the slope of the detuning at zero coupling indicates regular (if negative) or anomalous (if positive) frequency synchronization. It is straightforward to calculate the value of  $\theta$  for the transition between FS and AFS

$$\theta_{cr} = \frac{B_-}{B_+} = \frac{\beta_1 - \beta_2}{\beta_1 + \beta_2}. \quad (7)$$

For the particular case treated here ( $\beta_1 = -0.75$  and  $\beta_2 = -0.9$ ), we have  $\theta_{cr} = -1/11 \approx -0.09$ , in perfect agreement with what is found numerically for the full CGLE model and reported in Fig. 1. That means that for  $\theta_{cr} < \theta \leq 1$ , we have regular FS. Conversely, in the range  $-1 \leq \theta < \theta_{cr}$ , we have AFS. Notice that Eq. (7) is not at all applicable to the case reported by us in Fig. 4(b) of Ref. [6], since the fundamental assumption at the basis of whole theoretical derivation from Eq. (2) to Eqs. (5) (the fact that the amplitude field is almost constant and bounded away from zero) loses validity insofar as one of the two coupled fields is there in the amplitude turbulent regime, with phase defects characterizing also its uncoupled ( $c=0$ ) evolution.

Finally, we compare the numerical integration of the SDE (5) and of the full CGLE (1). In Fig. 3 we report the frequencies  $\Omega_1, \Omega_2$  versus the coupling strength  $c$  for two asymmetric coupling configurations. Namely, Fig. 3(a) [Fig. 3(b)] re-

fers to the case of regular FS at  $\theta = 0.88$  (of AFS at  $\theta = -0.88$ ). The agreement between the SDE (5) and the full CGLE (1) is very good at low coupling strengths. However, for larger values of  $c$ , we observe an increasing difference between the two cases, which is especially pronounced in the case of AFS. In particular, the full CGLE shows an enhancement of the anomaly with respect to the SDE (5).

In order to identify the reasons for such a difference, we point out that the derivation of the reduced SDE model is rigorous only in the absence of coupling. While one can reasonably expect that the validity of such reduction would hold also for small values of  $c$ , at larger coupling strengths intrinsic spatial effects become dominant in the dynamics of the coupled fields. In particular, even though initially the two fields are set in PT regimes, an intermediate coupling induces the presence of a finite number of phase defects [points

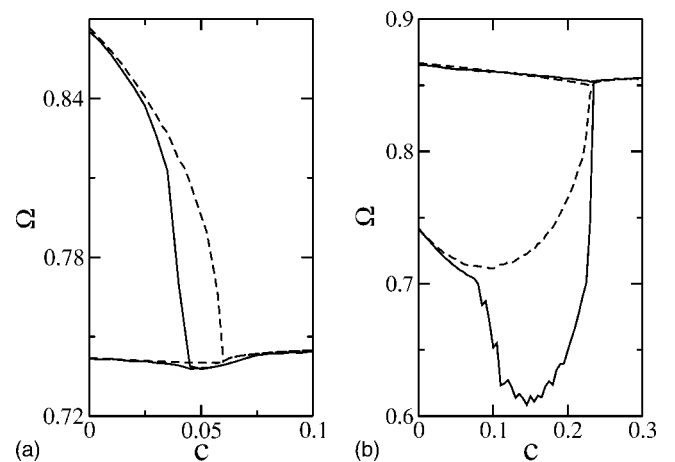


FIG. 3. Mean frequencies  $\Omega_{1,2}$  calculated for the full CGLE (1) (solid line) and the effective SDE (5) model (dashed line). (a)  $\theta = 0.88$  (regular FS). (b)  $\theta = -0.88$  (AFS) ( $\beta_1 = -0.75$ ,  $\beta_2 = -0.9$ ).

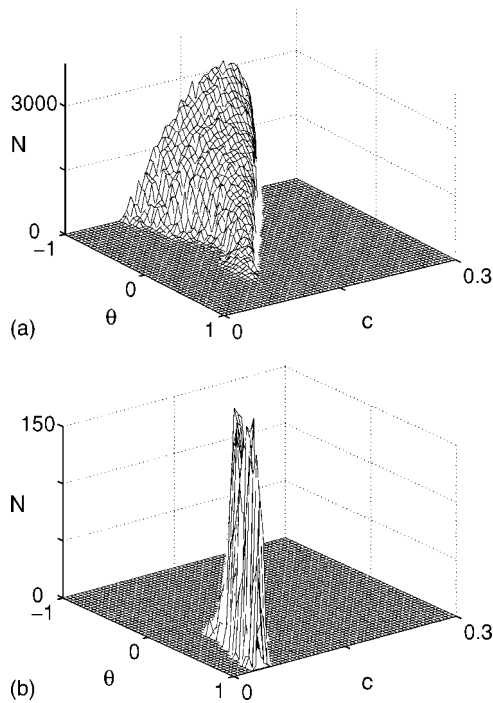


FIG. 4. Total number of defects  $N$  generated in Eq. (1) in the system (a)  $A_1$  and (b)  $A_2$  vs the parameter space  $(c, \theta)$ . Other parameters are  $\alpha=2$ ,  $\beta_1=-0.75$ ,  $\beta_2=-0.9$ . The defects at time  $t$  have been considered at those points  $x_i$ , where the  $\rho(x_i, t)$  is smaller than  $2.5 \times 10^{-2}$  and that are, furthermore, local minima for the function  $\rho(x, t)$ .

where locally and instantaneously the amplitude  $\rho(x, t)$  vanishes], as it appears from Fig. 4. Phase defects are objects inherent to the spatially extended nature of the system and cannot be retrieved in a SDE model. Notice that the small parameter mismatch ( $|\beta_1 - \beta_2| = 0.15$ ) guarantees the validity of the phase description (5) and hence the appearance of phase defects in the spatially extended system (1) cannot be related with the phenomenon of amplitude death occurring between two coupled limit cycle oscillators [14]. Indeed, in the above derivation, one has to implicitly assume the dynamical regime of the CGLE to be in phase turbulence. Therefore, the appearance of defects induce a breaking up of the validity of the reduced model (5).

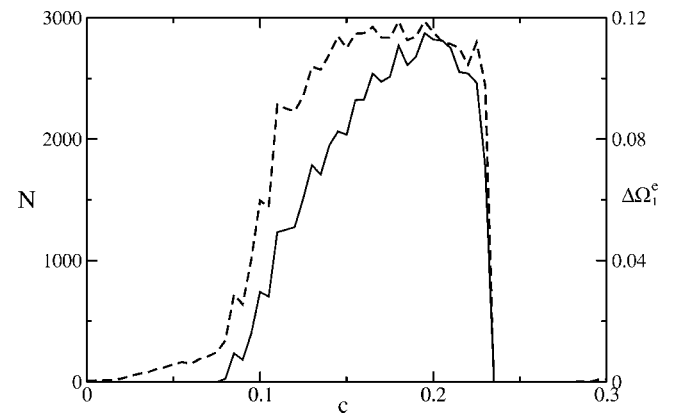


FIG. 5. Number of defects in system 1 (solid line—left ordinate) and frequency mismatch  $\Delta\Omega_1^e$  (dashed line—right ordinate, see text for definition) vs  $c$  for  $\theta=-0.88$  (AFS).

Phase defects are entirely responsible for the frequency mismatch observed in Fig. 3. Calling  $\Omega_1^{eff}$  ( $\Omega_1$ ) the mean frequency of system 1 as calculated with reference to the SDE model (the full CGLE model), in Fig. 5 we show that for  $\theta=-0.88$  (AFS), the 1:1 correlation between the frequency mismatch  $\Delta\Omega_1^e = \Omega_1^{eff} - \Omega_1$  and the number of defects appearing in system 1 is indeed remarkable, indicating that a simple correction of the frequency proportional to the defect numbers is enough to produce an excellent agreement between the SDE and the full CGLE models for the whole range of  $c$ .

In summary, the comparison between two time-dependent oscillators and spatially extended oscillators cannot be conducted without taking high care of phase defects. These last objects are inherent to space extended systems and must be taken into account if we want to study synchronization. In particular, AFS is further enhanced by phase defects, while in the case of regular FS, the presence of defects shifts down the threshold for synchronization, allowing for an easier frequency locking.

This work is partly supported by EU Contract No. HPRN-CT-2000-00158 (COSYC of SENS), MIUR-FIRB Project No. RBNE01CW3M-001, and MCYT Project (Spain) No. BFM2002-02011 (INEFLUID).

- [1] For a comprehensive review on the subject see: S. Boccaletti, J. Kurths, G. Osipov, D. Valladares, and C. Zhou, *Phys. Rep.* **366**, 1 (2002), and references therein.
- [2] S. Strogatz, *Sync: The Emerging Science of Spontaneous Order* (Hyperion Press, New York, 2003).
- [3] E. Montbrió and B. Blasius, *Chaos* **13**, 291 (2003).
- [4] B. Blasius, E. Montbrió, and J. Kurths, *Phys. Rev. E* **67**, 035204(R) (2003).
- [5] M. Cross and P. Hohenberg, *Rev. Mod. Phys.* **65**, 851 (1993).
- [6] J. Bragard, S. Boccaletti, and H. Mancini, *Phys. Rev. Lett.* **91**, 064103 (2003).
- [7] B. I. Shraiman, A. Pumir, W. von Saarloos, P. C. Hohenberg, H. Chaté, and M. Holen, *Physica D* **57**, 241 (1995).
- [8] Y. Kuramoto and T. Tsuzuki, *Prog. Theor. Phys.* **55**, 356 (1976).
- [9] Y. Kuramoto, *Prog. Theor. Phys. Suppl.* **64**, 346 (1978); G. I. Sivashinsky, *Acta Astronaut.* **4**, 1177 (1977).
- [10] H. Sakaguchi, *Prog. Theor. Phys.* **84**, 792 (1990).
- [11] C. Mendoza, Ph.D. thesis, University of Navarre, 2003 (unpublished).
- [12] E. Helfand, *Bell Syst. Tech. J.* **58**, 2289 (1979); H. Greenside and E. Helfand, *ibid.* **60**, 1927 (1981).
- [13] J. García-Ojalvo, J. M. Sancho, and L. Ramírez-Piscina, *Phys. Rev. A* **46**, 4670 (1992).
- [14] D. G. Aronson, G. B. Ermentrout, and N. Kopell, *Physica D* **41**, 403 (1990).